JOURNAL OF MATERIALS PROCESSING TECHNOLOGY 208 (2008) 423–430

journal homepage: www.elsevier.com/locate/jmatprotec

Influence of secondary electro-conductive phases on the electrical discharge machinability and frictional behavior of ZrO_2-based ceramic composites

K. Bonny[a,*], *P. De Baets*[a], *J. Vleugels*[b], *A. Salehi*[b], *O. Van der Biest*[b], *B. Lauwers*[c], *W. Liu*[c]

[a] *Ghent University (UGent), Department of Mechanical Construction & Production, IR04, Sint-Pietersnieuwstraat 41, B-9000 Gent, Belgium*

[b] *Catholic University Leuven (K.U. Leuven), Department of Metallurgy & Materials Engineering, MTM, Kasteelpark Arenberg 44, B-3001 Leuven, Belgium*

[c] *Catholic University Leuven (K.U. Leuven), Department of Mechanical Engineering, PMA, Celestijnenlaan 300 B, B-3001 Leuven, Belgium*

ARTICLE INFO

Article history:
Received 26 August 2007
Received in revised form
27 September 2007
Accepted 6 January 2008

Keywords:
ZrO_2 composite
Wire EDM
Material removal rate
Surface integrity
Dry sliding
Friction coefficient

ABSTRACT

ZrO_2-based composites with 40 vol.% WC, TiCN or TiN were processed in order to investigate the wire electrical discharge machining (EDM) possibility in demineralised water. The relationships between material removal rate (MRR), surface finish and wire EDM parameters were derived. Tribological data were obtained on wire-EDM'ed ZrO_2-based composites in reciprocating sliding contact with WC/Co cemented carbide using a pin-on-plate testing rig. Correlations between coefficient of friction on the one hand and material properties and test conditions on the other hand were determined. The experimental results revealed a strong influence of the secondary electro-conductive phase on the EDM behavior, surface finish, mechanical properties and frictional characteristics of the ZrO_2-based composites.

1. Introduction

In the aerospace, automotive and tool field, advanced ultra-hard materials with a high erosion/friction-resistance and high-temperature resistance are essential. However, these advanced materials, such as engineering ceramics, are normally difficult to machine with traditional techniques and can only be machined with high cost diamond and cubic boron nitride grinding tools. In addition, a higher cost for machining these materials would be expected. The technology of electrical discharge machining (hereafter EDM), on the other hand, is a non-conventional non-mechanical contact machining technology that is widely employed for electrically conductive materials, irrespective of their hardness. Moreover, the technique of EDM allows to machine intricate parts. However, engineering ceramics such as ZrO_2, Al_2O_3 or Si_3N_4 cannot be machined by EDM due to their too high electrical resistivity. In order to use the advantages of the EDM process, a secondary electrically conductive phase, such as WC, TiCN, TiB_2, ZrC, or TiN can be added to obtain a composite that is electrically con-

* *Corresponding author*. Tel.: +32 4 85 52 30 04; fax: +32 9 2 64 32 95.
E-mail address: koenraad.bonny@UGent.be (K. Bonny).
0924-0136/$ – see front matter © 2008 Elsevier B.V. All rights reserved.
doi:10.1016/j.jmatprotec.2008.01.020

ductive enough to allow EDM machining (Konig et al., 1988; Martin et al., 1989; Pitman and Huddleston, 2000; Kozak et al., 2004; Lauwers et al., 2005, 2004; McGeough, 1988).

This paper focuses on electrically conductive ZrO_2-based composites with TiN, $TiC_{0.5}N_{0.5}$ or WC addition. The EDM machinability of the zirconia composites was investigated and the differences are explained in terms of the ceramic composition. The material removal rate (MRR), surface integrity and surface roughness were assessed for 1 rough EDM cut and 4 consecutive finishing cuts. The frictional characteristics of wire EDM finished ZrO_2-based composites against WC-Co cemented carbide were investigated using dry reciprocating sliding experiments, in light of the scarce availability of published information on the tribological behavior of these ceramics (Terheci et al., 1996; Jahanmir, 1995). Correlations between coefficient of friction on the one hand, and microstructural and mechanical properties and test conditions on the other hand, were elucidated.

2. Experimental procedure

2.1. ZrO_2-based composites

The zirconia-based ceramic composites were obtained by hot pressing of yttria-stabilised ZrO_2 powder mixtures with 40 vol.% of WC, TiCN or TiN. The hot pressed discs were 42 mm in diameter and 5 mm thick. More information on the processing and characterisation of the ZrO_2-based composites is given elsewhere (Vleugels and Van der Biest, 1999; Salehi et al., 2006; Anné et al., 2005; Jiang et al., 2007).

The mechanical and physical properties of these ceramics are listed in Table 1. The composites should be suitable for EDM since their electrical resistivity is lower than $10^{-5}\,\Omega\,m$ (Konig et al., 1988). The investigated composites cover a wide range of material properties. The ZrO_2-WC composite combines an excellent strength, high toughness and high hardness. The ZrO_2-TiCN composite has a lower strength, lower toughness as well as lower hardness and the ZrO_2-TiN has the lowest toughness and hardness of the investigated ceramics, whereas the strength is comparable to that of the ZrO_2-TiCN material. Representative scanning electron micrographs of the different ceramic composites are shown in Fig. 1. The grain size distribution of the TiN and TiCN phase is comparable, but significantly coarser than that of the WC phase which was obtained from nanocrystalline WC starting powder.

2.2. Electrical discharge machining

All investigated ZrO_2-based ceramics were manufactured on a ROBOFIL 2000 (Charmilles Technologies, Switzerland) in demineralised water (dielectric conductivity 5 μS/cm), using a brass wire (CuZn37) electrode with a diameter of 0.25 mm and a tensile strength of 500 MPa. Initial rough cutting was performed to get a high MRR. In order to improve the surface quality, 4 consecutive finishing cuts were applied with lower energy input and a shorter duration of the applied energy pulses. The surfaces were observed by scanning electron microscopy (SEM, XL-30 FEG, FEI, The Netherlands). The wire EDM parameters and surface characteristics for the rough (R1) and 4 different finish cutting (F1–F4) regimes are summarised in Table 2.

2.3. Wear testing

The frictional behavior of wire-EDM'ed zirconia-based ceramics was evaluated using a high frequency tribometer (Plint TE77), in which a WC-Co cemented carbide pin was reciprocally slid against a ZrO_2-based composite counter plate, in an air-conditioned atmosphere of 23 °C and a relative humidity of 60%, in accordance with ASTM G133. The physical and mechanical properties of the pin material (CERATIZIT grade MG12 cemented carbide with 6 wt.% Co) are summarized in Table 3.

A schematic of the pin is outlined in Fig. 2. The top surfaces of the WC-Co pins were measured using surface scanning equipment (Somicronic® EMS Surfascan 3D, type SM3, needle type ST305), in order to derive an average surface topography and roughness profile. From these measurements, the average rounding radius and surface rough-

Table 1 – Physical and mechanical properties of the ZrO_2-based composites

Secondary phase[a]	E (GPa)	HV_{10} (kg/mm^2)	K_{IC} (MPa m$^{1/2}$)	3-Point bending strength (MPa)	Density (g/cm^2)	Resistivity ($10^{-6}\,\Omega$ m)
WC (20–40 nm)	328	1691 ± 8	8.5 ± 0.4	1964 ± 88	9.80	4.3
TiCN (1.6 μm)	284	1422 ± 10	7.0 ± 0.2	1521 ± 61	5.76	17.0
TiN (0.8–1.2 μm)	274	1370 ± 7	5.6 ± 0.1	1674 ± 314	5.81	4.6

[a] The number indicates the crystal size of the secondary phase starting powders.

Table 2 – Wire EDM parameters for rough (R1) and 4 finer (F1–F4) cutting regimes

EDM parameter	R1	F1	F2	F3	F4
Gap voltage (V)	−80	−200	−160	−120	+120
Pulse duration, t_e (μs)	2.4	0.4	1.2	1.2	0.4
Pulse interval, t_0 (μs)	20	10	4.3	5	4
Reference servo voltage, Aj (V)	60	150	55	27	0
Maximum current, I (A)	350	80	8	4	4
Ignition current height IAL (A)	5	7	7	5	5
Flushing pressure (bar)	8	0	0	0	0
Wire tension (N)	10	12	12	12	12
Wire winding speed (mm/min)	10	8	8	8	8
Material removed (μm)	–	16	11	7	0

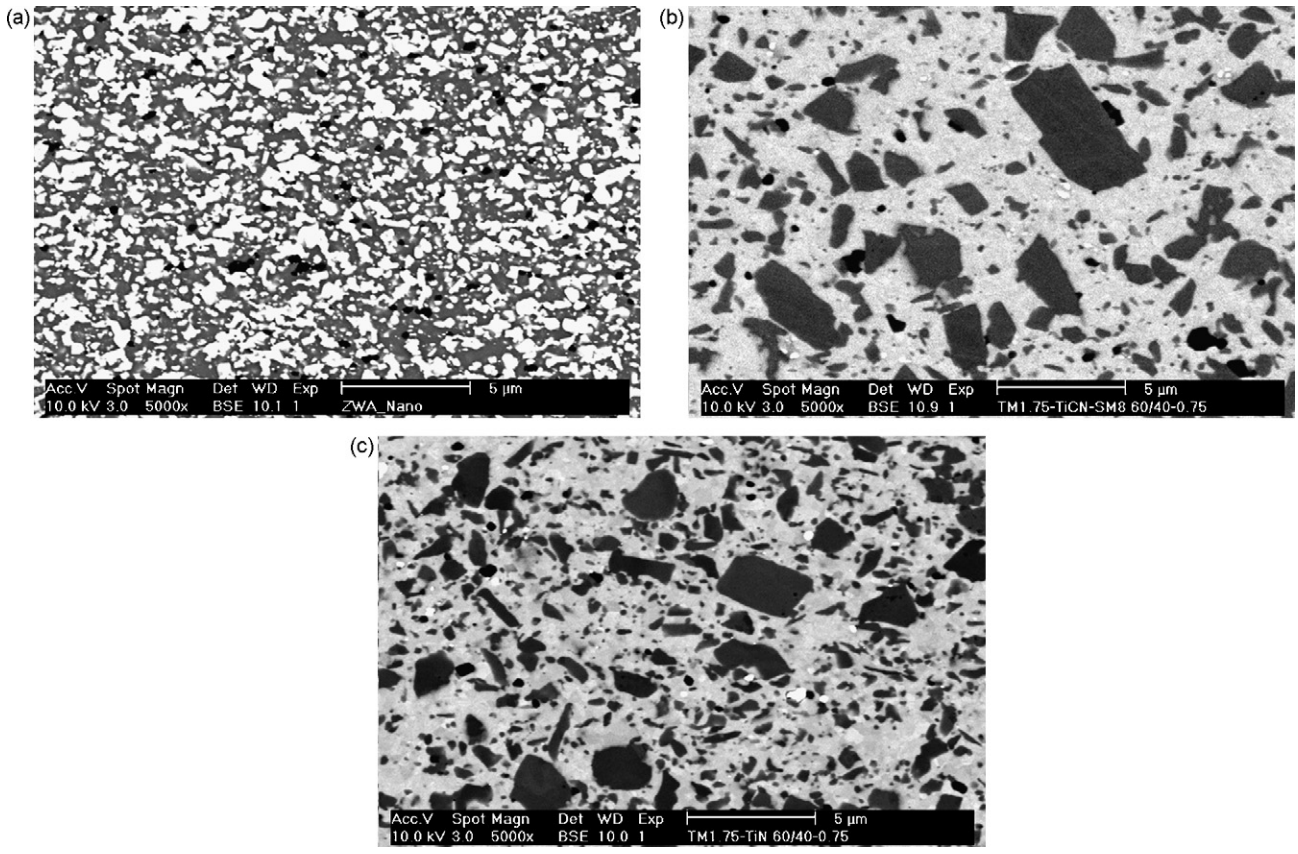

Fig. 1 – Microstructure of the ZrO_2-based composites with 40 vol.% WC (a), TiCN (b) and TiN (c) secondary electrically conductive phase addition.

Table 3 – Physical and mechanical properties of the WC-Co pin

Property	Value
Average WC grain size (μm)	0.55
Compressive strength (MPa)	7200
3-Point bending strength (MPa)	3078 ± 295
Vickers hardness HV_{10} (kg/mm^2)	1913 ± 13
Fracture toughness (MPa m$^{1/2}$)	9.3
Young's modulus, E (MPa)	609 ± 4
Thermal conductivity, K (W m^{-1} K^{-1})	90

ness R_a and R_t were determined to be 4.08 mm, 0.35 μm and 2.68 μm, respectively, Table 4. The contact load was varied from 15 N up to 35 N, with a 15 mm stroke length of the oscillating motion. A sliding velocity of 0.3 m/s was applied. The test duration was associated with a sliding distance of 10 km.

3. Results and discussion

3.1. *Material removal rate*

During testing, the gap voltage was fixed at −80 V, with a pulse interval time of 20 μs and a maximum discharge current of 350 A. Fig. 3 presents the correlation between MRR and pulse duration during rough wire EDM cutting of the ZrO_2-based composites, revealing that the MRR increases with increasing pulse duration in a perfect quadratic function. The following equations are obtained, Eqs. (1)–(3):

$$MRR_{WC} = -1.6607t_e^2 + 19.016t_e - 0.432, \quad R^2_{WC} = 0.9939 \qquad (1)$$

$$MRR_{TiCN} = -5.4029t_e^2 + 26.265t_e - 7.4327, \quad R^2_{TiCN} = 0.9974 \qquad (2)$$

$$MRR_{TiN} = -2.5052t_e^2 + 17.685t_e - 1.105, \quad R^2_{TiN} = 0.9893 \qquad (3)$$

Table 4 – Rounding radius, R_a and R_t, for 5 different pristine WC-Co pins

Pin	1	2	3	4	5	Average
Rounding radius (m)	4073.16	4079.22	4097.63	4070.64	4077.48	4080
R_a (m)	0.369	0.265	0.389	0.362	0.382	0.35
R_t (m)	1.755	1.617	2.212	4.101	3.69	2.68

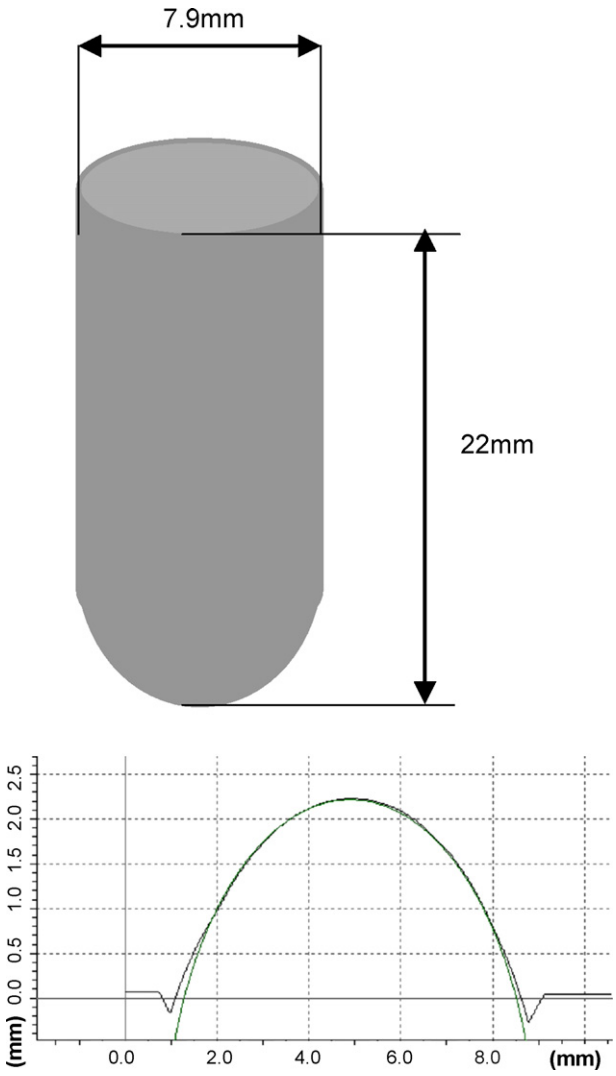

Fig. 2 – Dimensions, surface scanning topographies and surface profile of WC-Co hardmetal pins.

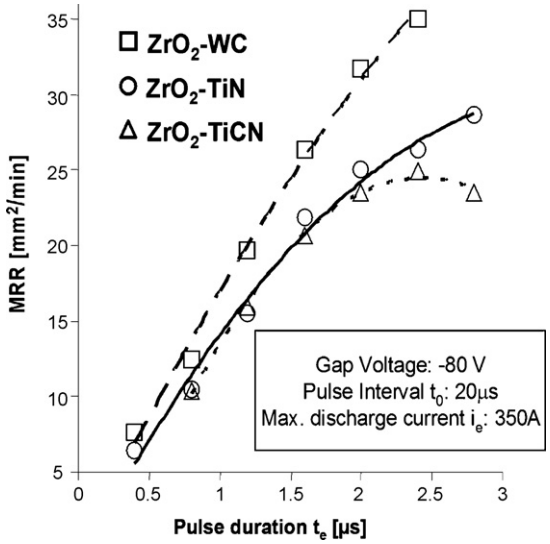

Fig. 3 – Relationship between MRR and pulse duration.

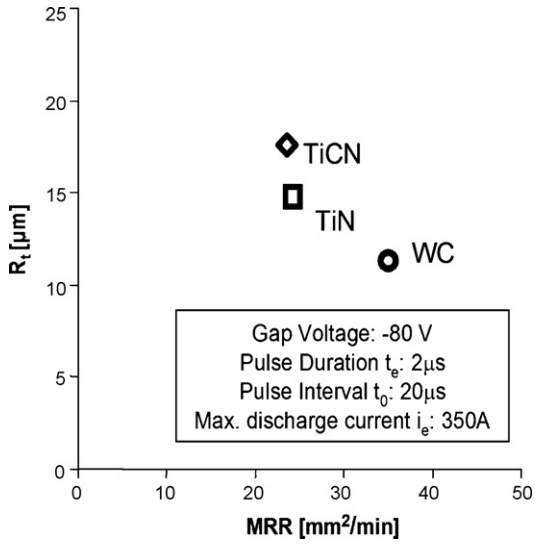

Fig. 4 – Correlation between MRR and surface roughness.

with MRR_{WC}, MRR_{TiCN} and MRR_{TiN} the material removal rates for the ZrO_2-WC, ZrO_2-TiCN and ZrO_2-TiN composites respectively and t_e the pulse duration. The *R*-square value, R^2, indicates that the equations perfectly match the experimental results.

Apparently, a peak value occurs in the quadratic function. The maximum MRR reaches up to 35.04 mm^2/min for the ZrO_2-WC composite at a pulse duration of 2.4 μs. At a pulse duration above 2.4 μs, the MRR intends to decrease until wire rupture, which terminates the wire EDM process. The correlation between MRR and pulse duration of the ZrO_2-TiCN and -TiN composites is similar as that of ZrO_2-WC. Actually, with increasing pulse duration, the sparking energy increases, which is beneficial for the MRR, but the probability of wire rupture increases as well. The experimental results revealed that the wire EDM process becomes unstable when exceeding a pulse duration of 2.4 μs, causing wire breakage.

The correlation between MRR and surface roughness is illustrated in Fig. 4, indicating that a similar but lower R_t, combined with a higher MRR can be accomplished for ZrO_2-WC composites. These trends should be attributed to the finer secondary phase and the lower thermal conductivity of ZrO_2-WC compared to ZrO_2-TiN and ZrO_2-TiCN composites.

3.2. *Surface integrity*

The topography of the rough cut (EDM regime R1) ZrO_2-WC composite processed with a gap voltage of −80 V, a pulse duration t_e of 2.4 μs, a pulse interval t_0 of 20 μs and a maximum discharge current i_e of 350 A (MRR: 35.04 mm^2/min) is shown in Fig. 5.

Both atomic number (BSE) and secondary electron (SE) micrographs reveal the presence of many droplets in clusters, voids, and a randomly distributed network of microcracks on the wire-EDM'ed surface. These phenomena indicate that the ZrO_2-WC ceramic is initially molten/evaporated by the sparking thermal energy during rough cutting. Most molten and oxidised material is flushed away from the gap by the

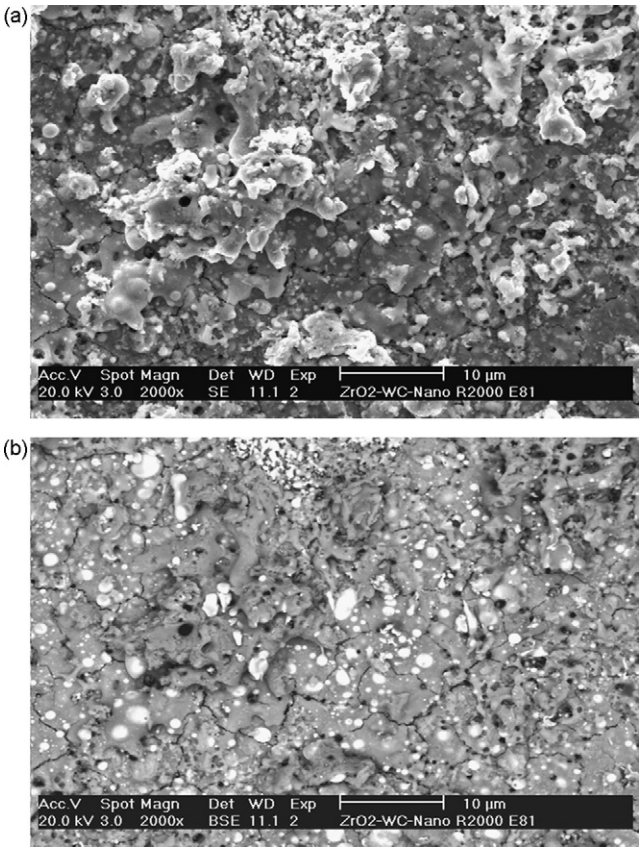

Fig. 5 – SE (a) and BSE (b) micrographs of the surface topography of rough cut ZrO_2-WC.

dielectric, whereas a small amount of melt resolidifies on the EDM surface to form clustered droplets. At the same time, the material on the surface will shrink in the process of resolidification after sparking due to the dielectric cooling. Due to the larger thermal expansion coefficient of the resolidified oxide layer compared to the composite substrate, microcracks are formed in the recast layer. Additionally, tensile residual thermal stresses can be expected in the surface layer of the composite material.

The rough cut wire-EDM'ed part does not meet the requirements for industrial applications because of the poor surface quality. In order to improve the wire-EDM'ed surface quality, several consecutive finish cuttings with decreasing sparking energy are carried out to remove the droplets, craters and microcracks on the surface. The surface and cross-sectioned views after rough and the finest finish cutting regime (F4: gap voltage, +120 V; pulse duration t_e, 0.4 μs; pulse interval t_0, 4 μs; maximum discharge current i_e, 4 A) are compared for the ZrO_2-WC composite in Fig. 6.

The average values of the surface roughness parameters R_a and R_t under rough and finish cutting regimes, are compared in Table 5 for the investigated ZrO_2-based ceramic composites. In all cases, R_a and R_t are noticed to exhibit a similar trend. It is obvious that the surface roughness becomes progressively lower after finish cuttings, because of the gradually lower sparking energy applied for the surface. For the ZrO_2-WC samples, for instance, the R_t-value decreased from 11.31 μm after rough cutting to 4.74 μm after the final finish cut. This implies that the large droplets, craters and microcracks left by previous cutting regimes have been almost completely removed, although a small amount of recast material remains even after the final finishing cut. As for the other ceramic composite systems, their surface integrities are similar to that of ZrO_2-WC, after both rough and finish cutting EDM regimes. No clearly defined heat affected zone induced by sparking thermal energy can be observed on the cross-sectioned wire-EDM'ed ceramic surfaces, for both rough and finish cutting, which is definitely different than when wire EDM'ing steel. This probably benefits from the ceramic properties, such as a higher melting point and lower thermal conductivity than that of steel, which strongly limits the extend of thermal damage.

Under equal set-up and identical series of EDM parameters, the ZrO_2-WC specimens obtain the smoothest surfaces, whereas the highest roughness values are encountered with the ZrO_2-TiCN ceramic composites. For ZrO_2-TiCN and ZrO_2-TiN composites, the EDM-regime F3 is noticed to yield slightly lower surface roughness than the final EDM-regime F4, i.e. R_t rising from 5.42 to 6.37 μm and from 4.90 to 5.16 μm, respectively, in contrast with the ZrO_2-WC composites, with R_t decreasing from 6.23 to 4.74 μm.

The surface roughness of the investigated ceramic composites after rough and finish cutting (EDM-regimes R1 and F4, respectively) are compared in Fig. 7, demonstrating that the best surface quality is obtained with the ZrO_2-WC composite, both for rough and finish cutting. This can be attributed to the lower grain size of the secondary phase in the ZrO_2-WC composites in comparison with the ZrO_2-TiN and ZrO_2-TiCN grades, as shown in Fig. 1.

Table 5 – Surface roughness R_a and R_t for the rough (R1) and smoother (F1–F4) EDM regimes employed on the ZrO_2-based composites

EDM-regime	Grade					
	ZrO_2-WC		ZrO_2-TiCN		ZrO_2-TiN	
	R_a (μm)	R_t (μm)	R_a (μm)	R_t (μm)	R_a (μm)	R_t (μm)
R1	1.44	11.31	2.34	17.67	2.07	14.77
F1	1.27	10.26	1.28	12.17	1.06	8.82
F2	1.09	8.61	0.80	7.93	0.84	7.04
F3	0.80	6.23	0.66	5.42	0.64	4.90
F4	0.57	4.74	0.70	6.37	0.65	5.16

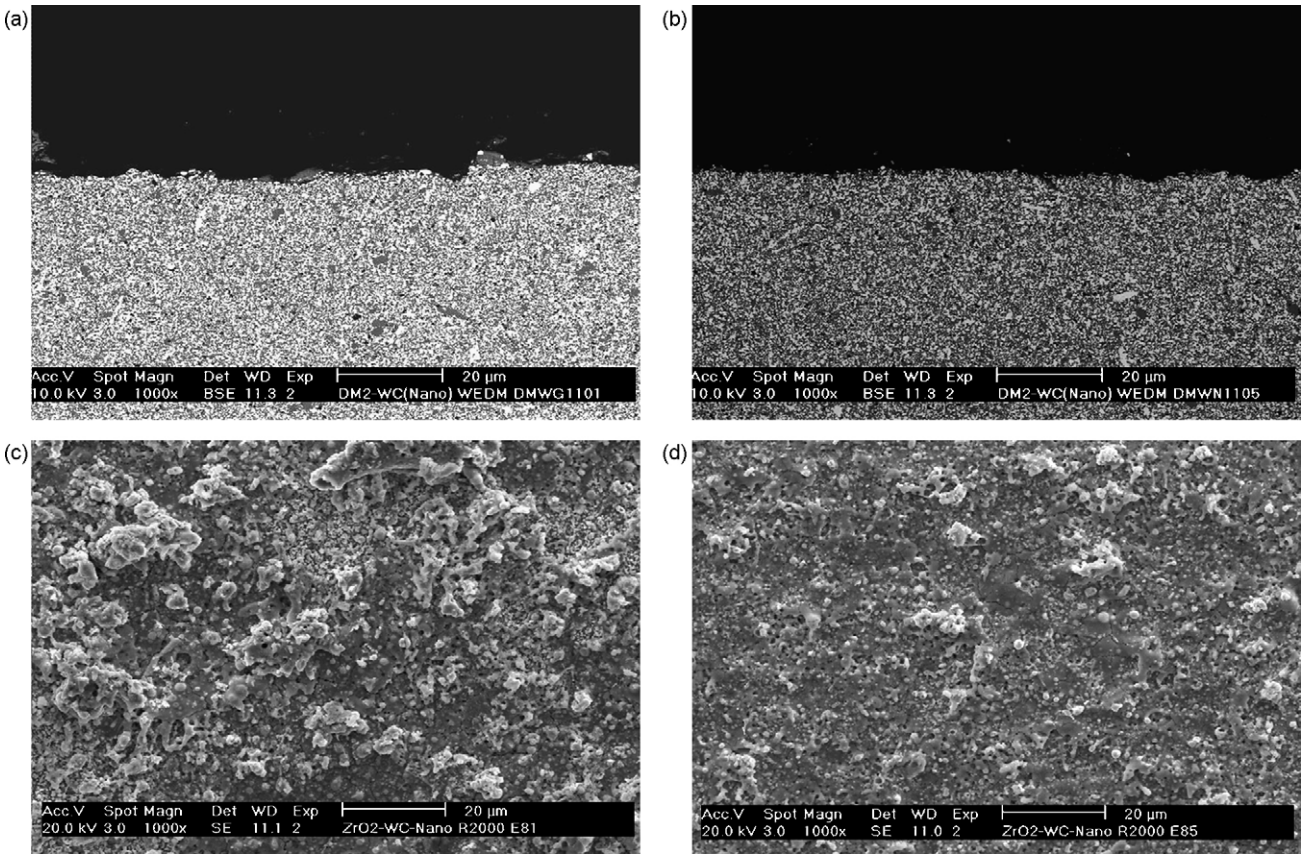

Fig. 6 – Cross-sectional views and topographies of the ZrO_2-WC composite after rough (a and c) and finest (b and d) cutting regime.

Based on the analysis of the topography and cross-sectional views, the wire-EDM material removal of ZrO_2-based ceramics appears to occur completely in agreement with the mechanism of melting/evaporation. No evidence of other mechanisms, such as spalling or thermal shock, was discovered in the process of wire EDM of ZrO_2-based ceramics (Lauwers et al., 2005, 2004). From the MRR and surface roughness viewpoint, the best performance is obtained for the ZrO_2-WC composites.

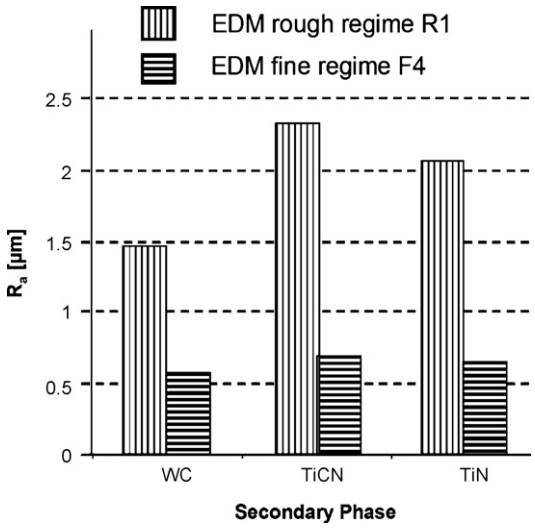

Fig. 7 – Surface roughness under rough and finest EDM regime for different secondary phase additions in ZrO_2-based composites.

3.3. *Frictional properties*

3.3.1. *Coefficient of friction (μ)*

Friction is a main representative of responses of a tribosystem. The applied normal force (F_N) and the concomitant tangential frictional force (F_T) of pin-on-flat sliding pairs were measured on-line using a load-cell, parallel with the lever of the loading frame, and a piezoelectric transducer, attached to the holder that supports the flat counterbody. The F_T/F_N forces ratio is defined as the coefficient of friction (μ), which can be differentiated in a static (μ_{stat}) and a dynamic component (μ_{dyn}). For each sliding wear experiment, a new WC-Co pin was used in order to ensure identical initial surface conditions.

Friction coefficient curves for the finish cut (EDM-regime F4) ceramic composite flat/WC-Co pin combinations as function of the oscillating sliding distance(s) are shown in Fig. 8. Each curve is an average of at least two wear experiments performed under identical conditions, with a standard deviation of less than 10% between different samples of the same material. The error bars indicating the extent of the variations are excluded to make the figure better readable.

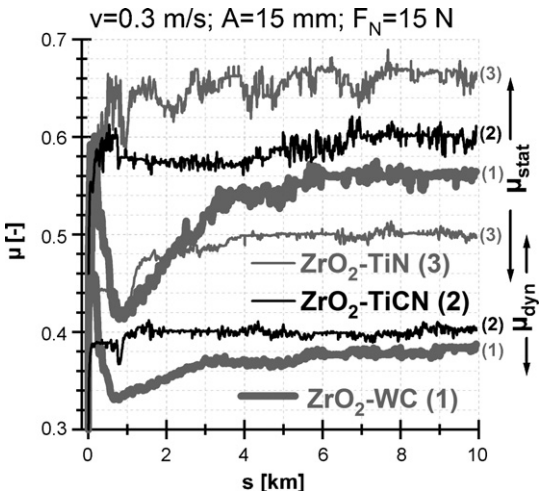

Fig. 8 – Static and dynamic friction coefficient curves for fine EDM (F4) ZrO_2 composite flat/WC-Co pin pairs sliding at 0.3 m/s, with a 15 N contact load.

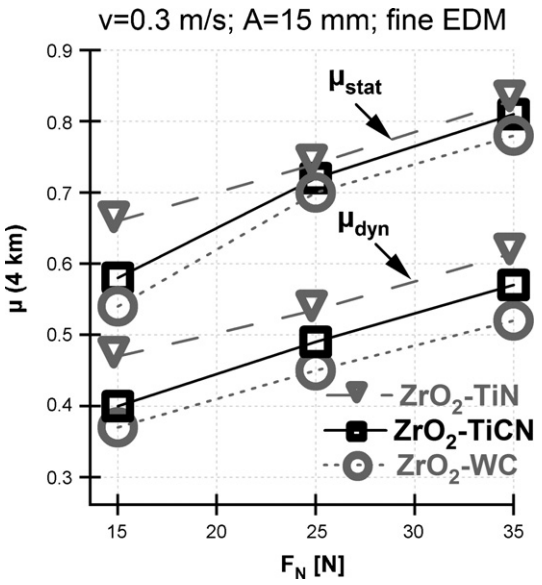

Fig. 9 – Steady-state friction coefficient vs. contact load for fine EDM (F4) ZrO_2 composite flat/WC-Co pin sliding pairs ($v = 0.3$ m/s, $s = 4$ km).

The friction coefficient of the investigated tribopairs was measured to be in the range of 0.38–0.68 and 0.33–0.51 for the static and dynamic component respectively. The dynamic and static component of friction are found to vary very similarly as function of the sliding distance, however at a different level. In all cases, the coefficient of friction is noticed to increase abruptly during the first meters of sliding and then gradually ascends further during the growing pin on plate contact surface and the concomitant removal of the recast surface layer. After a running-in stage, the friction coefficient drops down shortly and rises again above its prior level. Beyond a sliding distance of 4 km, the variations in the friction force curve are marginal. Therefore, a steady state coefficient of friction can be represented by an averaged value over the sliding distance between 4 and 10 km.

The temporary drop down followed by a steep increase in friction coefficient corresponding with a wear path length of approximately 1 km has not been fully elucidated and probably represents an edge phenomenon. However, the instabilities in the friction curves during the first sliding kilometers can be related with the changes in the sliding contact surface as a result of the removal of the wire-EDM induced recast layer.

The instabilities in the friction curves, during running-in stage as well as in steady state, are due to a continuous breaking and regeneration of micro junctions as a result of asperity interaction and should be related to the constantly changing degree of adhesion between the contact surfaces (Jahanmir, 1995). The static and dynamic friction coefficient display a similar evolution as function of the sliding distance, however at a different level. The fluctuations in friction occur globally with higher amplitude for the static component compared to its dynamic equivalent.

The effect of the secondary phase material on the friction coefficient is quite pronounced. The lowest friction level is encountered with the ZrO_2-WC ceramic composite, whereas the ZrO_2-TiN specimens exhibit the highest coefficient of friction. Moreover, the friction curve progression of the ZrO_2-WC composite, i.e. (i) a high initial friction level, followed by (ii) a sharp descent and (iii), a gradual increase to a more or less constant value after a sliding distance of about 1 km, differs from the other ZrO_2 composite grades. Some numerical data are provided in Table 6, in which friction coefficients at various sliding distance are listed for the investigated tribopairs.

3.3.2. *Influence of contact load*

Comparative dry reciprocating sliding wear experiments using distinctive normal loads (15, 25 and 35 N) were performed in order to investigate correlations between contact conditions and frictional characteristics. The dependency of the steady state coefficient of friction (μ) on the applied contact load (F_N) is compared for all fine-EDM'ed zirconia-based composites in Fig. 9.

Table 6 – Static and dynamic friction coefficient as function of sliding distance for the EDM finished (regime F4) ZrO_2 composite flat/WC-Co pin pairs ($v = 0.3$ m/s; $F_N = 15$ N)

	μ_{stat}				μ_{dyn}			
Wear path (km)	0.045	1	4	10	0.045	1	4	10
ZrO_2-WC	0.59	0.44	0.52	0.54	0.44	0.36	0.38	0.39
ZrO_2-TiCN	0.55	0.57	0.58	0.59	0.39	0.39	0.40	0.40
ZrO_2-TiN	0.54	0.61	0.66	0.66	0.40	0.43	0.48	0.49

Within the applied contact load range, the static coefficient of friction is noticed to vary between 0.54 and 0.83, whereas values between 0.37 and 0.63 were recorded for the dynamic component. In all cases, the coefficient of friction, obtained after a wear path length of 4 km, is noticed to increase with increasing contact load. Consistent with the frictional behavior, observed in Fig. 8, the highest steady state level of friction was encountered with the ZrO_2-TiN samples, whereas the ZrO_2-WC composite displays the lowest degree of friction. The difference between the composites, however, is noticed to decrease with increasing contact load.

4. Conclusions

ZrO_2-based composites with 40 vol.% WC, $TiC_{0.5}N_{0.5}$ or TiN phase addition have proven to be appropriate for wire EDM in demineralised water. The material removal mechanism was full melting and evaporation. Although the surface quality was modest after rough EDM cutting, with the formation of a recast layer, containing many resolidified droplets and voids as well as a microcrack network, the surface roughness could be reduced from about 18 μm R_t or 2.5 μm R_a after rough EDM down to 6 μm R_t or 0.7 μm R_a after 4 consecutive EDM finish cutting regimes. Amongst the ZrO_2-based composites, ZrO_2-WC exhibited better performance in EDM machinability (MRR and surface quality) and higher mechanical properties (strength, hardness and toughness), compared to ZrO_2-TiN and ZrO_2-TiCN composites with equal volumetric secondary phase content. The considerable impact of the secondary phase was reflected in the dry reciprocating frictional behavior against WC-Co cemented carbide. The most favorable tribological results were obtained for ZrO_2-WC composites. A rising contact load was found to increase the friction coefficient.

Acknowledgements

This work was co-financed by the Flemish Institute for the promotion of Innovation by Science and Technology in industry (IWT) under project contract number GBOU-IWT-010071-SPARK. The authors gratefully recognize all support, scientific contributions and stimulating collaboration from the investigation partners from Ghent University (UGent) and Catholic University of Leuven (K.U. Leuven). Special appreciation goes to CERATIZIT for supplying the cemented carbide pins.

REFERENCES

Anné, G., Put, S., Vanmeensel, K., Jiang, D., Vleugels, J., Van der Biest, O., 2005. Hard, tough and strong ZrO_2-WC composites from nanosized powders. J. Eur. Ceram. Soc. 25 (1), 55–63.

Jahanmir, S., 1995. Friction and wear of ceramics. Tribol. Int. 28 (6), 421–427.

Jiang, D., Van der Biest, O., Vleugels, J., 2007. ZrO_2-WC nanocomposites with superior properties. J. Eur. Ceram. Soc. 27, 1247–1251.

Konig, W., Dauw, D.F., Levy, G., Panten, U., 1988. EDM–future steps towards the machining of ceramics. Ann. CIRP 37, 623–631.

Kozak, J., Rajurkar, K.P., Chandarana, N., 2004. Machining of low electrical conductive materials by wire electrical discharge machining (WEDM). J. Mater. Proc. Tech. 149 (1–3), 266–271.

Lauwers, B., Kruth, J.-P., Liu, W., Eeraerts, W., Schacht, B., Bleys, P., 2004. Investigation of material removal mechanisms in EDM of composite ceramic materials. J. Mater. Proc. Tech. 146 (1–3), 347–352.

Lauwers, B., Liu, W., Kruth, J.P., Vleugels, J., Jiang, D., Van der Biest, O., 2005. Wire EDM machining of Si_3N_4-, ZrO_2- and Al_2O_3-based ceramics. Int. J. Electr. Machining 10, 33–37.

Martin, C., Cales, B., Vivier, P., Mathieu, P., 1989. Electrical discharge machinable ceramic composites. Mater. Sci. Eng. A109, 351–356.

McGeough, J.A. (Ed.), 1988. Advanced Methods of Machining. Chapman and Hall.

Pitman, A., Huddleston, J., 2000. Electrical discharge machining of ZrO_2/TiN particulate composite. Br. Ceram. Trans. 99, 77–84.

Salehi, S., Van der Biest, O., Vleugels, J., 2006. Electrically conductive ZrO_2-TiN composites. J. Eur. Ceram. Soc. 26, 3173–3179.

Terheci, M., Nanos, J., Giannakoudaris, H., Abanteriba, S., 1996. Tribological behavior of yttria-stabilised zirconia under dry sliding conditions when tested against itself and grey automotive cast iron. Wear 201, 26–37.

Vleugels, J., Van der Biest, O., 1999. Development and characterization of Y_2O_3-stabilized ZrO_2 (Y-TZP) composites with TiB_2, TiN, TiC and $TiC_{0.5}N_{0.5}$. J. Am. Ceram. Soc. 82, 2717–2720.